# Chapter 6
# Fundamental Characterization of Epoxy-Silica Nanocomposites Used for the Manufacturing of Fiber Reinforced Composites

**Thorsten Mahrholz and Michael Sinapius**

**Abstract** Nanocomposites based on silica nanoparticles and high performance epoxy resins are investigated for their suitability as a new type of matrix for fiber-reinforced polymers (FRP) using injection technologies (LCM). The key focus is on the determination of the processing parameters at varying silica nanoparticle content. The homogeneous distribution of the nanoscaled silica in the epoxy matrix is proven by photon cross correlation spectroscopy (PCCS) and scanning electron microscopy (SEM) analysis. Depending on the silica content of the composite, its stiffness, strength and toughness can be increased significantly compared with the neat resin. The mechanical performance is discussed by failure mechanisms based on the analysis of the fracture surface morphology. Moreover, resin shrinkage and the thermal expansion are significantly reduced both important for lowering internal stress in FRP. The injectability of the nanocomposite for the purpose of lamination using the LCM technology is nearly unaffected. Epoxy-silica nanocomposites are now proven to be a new high performance polymer matrix for FRP structures manufactured by the low cost LCM techniques.

## 6.1 Introduction

Prepreg technology is currently the most widely used manufacturing technique for making high performance fiber composites (FRP). Despite good composite quality, this manufacturing technique carries the disadvantages of high manufacturing

T. Mahrholz (✉) · M. Sinapius
Institute for Composite Structures, German Aerospace Center DLR, Lilienthalplatz 7, 38108, Braunschweig, Germany
e-mail: thorsten.mahrholz@dlr.de

M. Wiedemann and M. Sinapius (eds.), *Adaptive, Tolerant and Efficient Composite Structures*, Research Topics in Aerospace, DOI: 10.1007/978-3-642-29190-6_6,

costs and minimal potential cost savings. Injection techniques (Liquid Composite Moulding—LCM), such as RTM, VARI, DP-RTM and SLI are alternative manufacturing techniques that have been developed in recent years [1–3] and are already in industrial application. Low manufacturing costs achieved through a combination of inexpensive resins and semi finished fiber materials are decisive advantages compared with the prepreg technology. However, the properties of high performance composites produced by LCM techniques have not yet reached the level of the Prepreg composites. This is essentially caused by the matrix shrinkage in the polymer system, which leads to internal stress reducing the material performance. Traditional microfillers which are investigated for reducing the matrix shrinkage lead to manufacturing problems i.e. increased viscosity and filtration effects and brittleness of the matrix. In order to avoid these problems so called nanocomposites i.e., thermosetting resins filled with nanoparticles (1–100 nm) are proposed.

In the present study nanoscaled silica particles produced in a sol–gel technique [4, 5] are focused on to eliminate main disadvantages of the LCM technology and, at the same time, to increase the material composite qualities. Espcially the thermal, mechanical and rheological properties of the nanocomposites are thoroughly studied. Moreover the influences of nanoparticles on the macroscopic properties of the polymer matrix are discussed with the fracture surface morphology as a reference. Finally the suitability of this new type of polymer matrix for manufacturing of fiber composite materials through injection technology is assessed. The long term objective of the investigation is to use nanoparticles for making tailored higher performance reaction resin available for the manufacturing of FRP by LCM techniques. The use of nanocomposites as a new type of polymer matrix will significantly improve the spectrum of properties of FRP, thus expanding the range of applications of fiber composite structures.

## 6.2 Materials and Preparation

The material used in this study is an epoxy resin, diglycidyl ether of bisphenol A (DGEBA) (Araldite LY556; Huntsman), cured by an anhydride curing agent, 4-methyl-1,2-cyclohexanedicarboxylic anhydride (Aradur HY917; Huntsman) and accelerated by an amine, 1-methyl-imidazole (DY070; Huntsman). The nanoparticle system is a commercially available spherical silica pre-dissolved in a bifunctional epoxy resin (similar to Araldite LY556). The master batch provided by Hanse-Chemie AG (Germany) consists of 40 wt% silica nanoparticles. These particles are manufactured by means of a sol–gel technique and grow directly in the polymer matrix [4, 6]. The primary particle size can be adjusted through quenching processes and is within a range of 8–50 nm (note of the producer). The particle surface was also modified by Hanse-Chemie AG with a reactive organic silane which allows a polymerisation directly with the resin matrix and prevents particle agglomeration.

**Table 6.1** Thermal parameters of the prepared epoxy-silica nanocomposites

| Sample | $SiO_2$ (wt%) | $\rho^a$ (g/cm$^3$) | $\Delta H^b$ (J/g) | $T_{g\ (DSC)}^b$ (°C) | $T_{g\ (DMA)}^c$ (°C) | HDT$^d$ (°C) | $\alpha^e_{T<Tg}$ ($10^{-6}$/K) | $\alpha^e_{T>Tg}$ ($10^{-6}$/K) |
|---|---|---|---|---|---|---|---|---|
| NA-0 | 0 | 1.209 | 384 | 130.8 | 126.1 | 116.8 | 62.0 | 184.0 |
| NA-5 | 5 | 1.235 | 369 | 132.3 | 127.5 | 118.3 | 58.4 | 180.3 |
| NA-15 | 15 | 1.286 | 324 | 127.4 | 126.2 | 116.4 | 54.7 | 171.1 |
| NA-25 | 25 | 1.340 | 280 | 127.9 | 122.6 | 112.5 | 45.8 | 158.9 |

[a] Specific gravity measured for the cured samples at 25°C
[b] Specific reaction enthalpy ($\Delta H$) and glass transition temperature ($T_g$) determined by DSC
[c] Glass transition temperature ($T_g$) determined by DMA (tan$\delta$)
[d] Heat distortion temperature determined as onset temperature from DMA curves
[e] Coefficient of thermal expansion (CTE) at various temperature ranges

The influence of the nanoscaled silica concentration on the range of properties of the epoxy matrix (Araldite LY type) was investigated in a series of tests in order to determine the best concentration range for FRP production. Therefore the master batch of silica (40 wt%) was first diluted with the neat epoxy resin and afterwards well mixed with the hardener and accelerator. In each case the mix ratio of the epoxy resin (Araldite LY556), the hardener (Aradur HY917) and the accelerator (DY070) was 100: 90: 0.5 wt%. The silica concentration was adjusted within a range of 0–25 wt%. After a short de-gassing process the mixture was poured into a pre-heated aluminium mould. The modified resins were pre-cured at 80°C for 4 h and post-cured at 120°C for 4 h. Cured samples were then cut and ground for mechanical testing. The filled and unfilled matrix resins were characterised extensively in terms of their thermal, rheological and mechanical properties. More details can be taken from a former published paper [7]. An overview of the prepared nanocomposites as well as the corresponding thermo-mechanical parameters is given in Tables 6.1 and 6.2.

## 6.3 Characterization of the Nanocomposites

### *6.3.1 Analysis of the Nanoparticle Distribution*

It is well known that the degree of dispersion of nanoparticles in a polymer matrix is a governing parameter which controls the final properties of the resulting nanocomposites. Only an extremely homogeneous particle distribution with the development of primary nanoparticles efficiently reinforces the polymer matrix. Thus, the quality of the dispersions manufactured as a mixture of the silica master batch, the neat epoxy resin, the anhydride hardener and accelerator are investigated for a broad range of silica content. The liquid and solid states are analyzed by means of photonen cross correlation spectroscopy (PCCS) and scanning electron microscopy (SEM), respectively. SEM images prove the homogeneous

**Table 6.2** Mechanical parameters of the prepared epoxy-silica nanocomposites

| Sample | $SiO_2$ | Tension test | | | Flexural test | | $G^a_{1c}$ | $K^a_{1c}$ |
|---|---|---|---|---|---|---|---|---|
| | (wt%) | $E_t$ (MPa) | $\sigma_t$ (MPa) | $\varepsilon_t$ (%) | $E_f$ (MPa) | $\sigma_f$ (MPa) | ($J/m^2$) | (MPa $m^{1/2}$) |
| NA-0 | 0 | 3359 | 88 | 3.26 | 3484 | 157 | 77 | 0.517 |
| NA-5 | 5 | 3526 | 91 | 4.51 | 3607 | 160 | 137 | 0.713 |
| NA-15 | 15 | 3978 | 95 | 5.10 | 4048 | 165 | 177 | 0.865 |
| NA-25 | 25 | 4555 | 98 | 4.40 | 4525 | 171 | 196 | 0.957 |

[a] Fracture toughness parameters: $G_{1c}$—critical energy release rate; $K_{1c}$—critical stress intensity factor

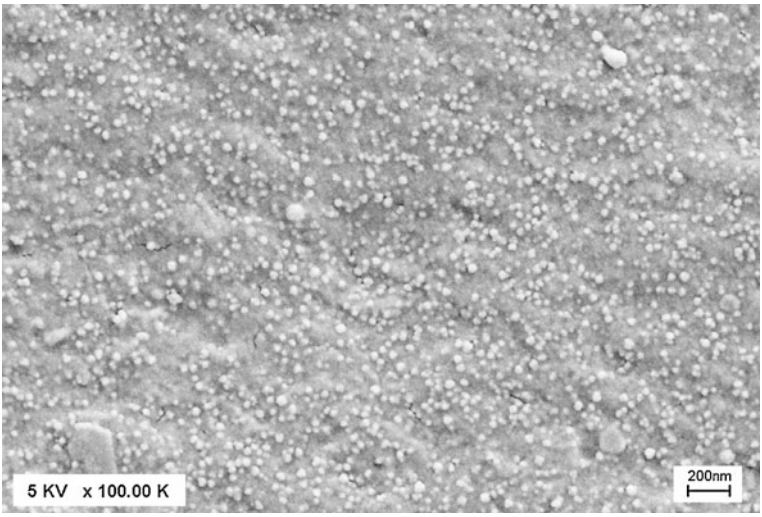


**Fig. 6.1** SEM image of a nanocomposite based on silica and epoxy resin (25 wt% silica). Surface prepared by cryoscopic fracture

distribution of the spherical silica particles in the cured nanocomposite as well as the absence of any major agglomeration of particles (see Fig. 6.1). The PCCS demonstrates the very narrow and monomodal particle size distribution (2–50 nm) with an average size of 16 nm in the liquid resin (Fig. 6.2). It is evident that a good dispersion quality is retained in the nanocomposite from the liquid to the fully cured state and that primary particles are obtained.

### *6.3.2 Rheological Properties*

The viscosity and resin gel-time are key factors for FRP structures manufactured by LCM. These factors determine the injectability of the resin and the fabric wetting process. Therefore, the flow behaviour of the nanocomposites are

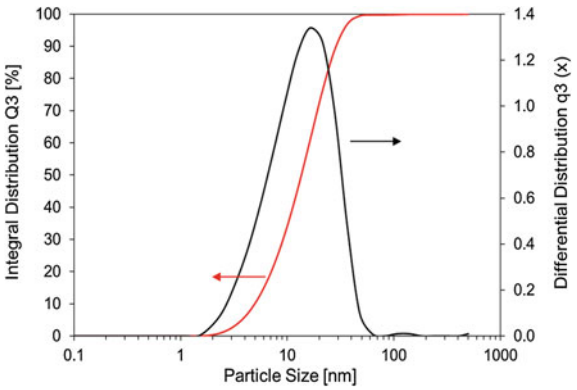


**Fig. 6.2** Differential and integral particle size distribution of 25 wt% silica nanoparticles in an epoxy resin determined by PCCS

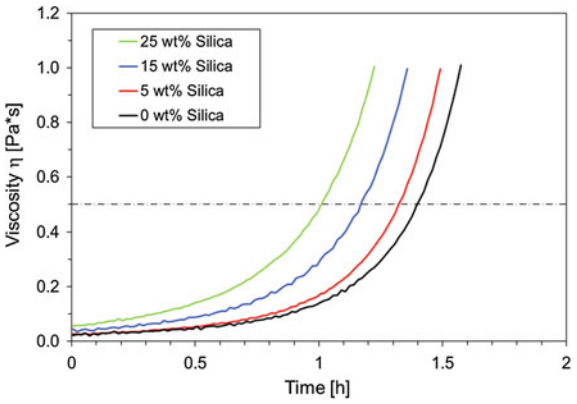


**Fig. 6.3** Dynamic viscosity of epoxy-silica nanocomposites as function of process time and varying silica contents (0–25 wt%). Conditions: 80°C and constant shear rate of 4 Hz. Limiting viscosity number for LCM is 0.5 Pa*s

investigated in a series of rheological experiments, increasing the filler content up to 25 wt% silica at a typical injection temperature of 80°C for the neat epoxy resin used. The limiting viscosity number for injection technology is normally in the range of 500 mPa*s. The time required to reach that limit is defined as pot life with respect to the injection technology used. The corresponding isothermal viscosity curves are depicted in Fig. 6.3.

Increasing the filler content under the described conditions leads to a reduction in pot life from 1.4 to 1 h. DSC measurements have shown that this is not due to any catalytic effects [7]. It is likely that the observed reduction in gel-time can be explained by a pure physiochemical effect. As the curing reaction progresses, long polymer chains develop which interact extensively with the large surface of the nanoparticles. This causes a disproportional increase in viscosity compared with the reference resin. However, with regard to the filler content studied herein, the reduction in pot life as well as the small increase of the initial viscosity are

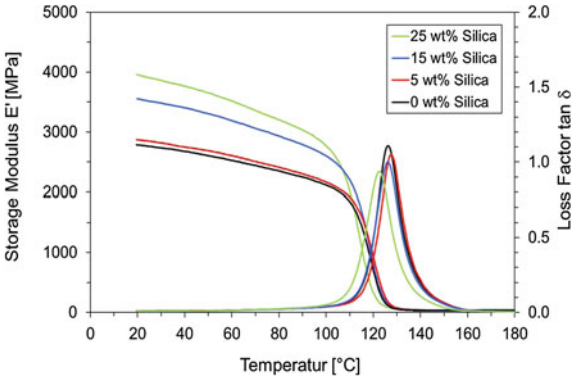


**Fig. 6.4** Storage modulus and loss factor of the epoxy-silica nanocomposites as a function of temperature and degree of silica filling measured by DMA (tension mode)

acceptable and are still in the range of processability for the LCM technique. The injectability is retained in the modified resins.

### *6.3.3 Thermal Characterization by DMA and DSC*

The heat distortion temperature (HDT) known as an important key driver for FRP was investigated for epoxy-silica nanocomposites in an extended temperature range measured by dynamic mechanical analysis (DMA). Here the HDT is defined as the onset temperature taken form the storage modulus E' by the tangent method. The glass transition temperature was analysed by the loss factor (tan$\delta$). The results are summarized in Table 1 and are depicted in Fig. 6.4.

Obviously the DMA data reveal a high influence of the content of silica nanoparticles on the stiffness (E') of the modified epoxy resin at a temperature below $T_g$, i.e. in the glassy state at about 20–100°C, while the modulus becomes almost indendent of the silica content at the glass transition state (ca. 120°C). Consequently the material properties in the glassy state are considerably determined by the nanoparticles. In the range of the glass transition a nanoparticle effect is no more clearly detectable i.e. above the onset temperature E' seems to be predominantly determined by the pure matrix properties. On the other hand the slightly reduced loss factors (tan$\delta$), indicating a lower damping behaviour, suggest an improved particle–matrix bonding [5] more discussed in Sect. 3.8. However, in terms of the nearly constant values of HDT the silica nanoparticles examined here do not enable an extension of the thermal field of applications.

Additionally, the glass transition temperature ($T_g$) was determined by DSC. The values of $T_g$ decrease slightly by 2% from 131 to 128°C by increasing the filler content up to 25 wt% silica (Table 6.1). Obviously, the used silica nanoparticles have only a slight influence on $T_g$ even at high degrees of filling. Interestingly the detected glass temperatures from the DSC show an amazingly good correlation with those ones from the DMA measurements (low shift of tan$\delta$). This also

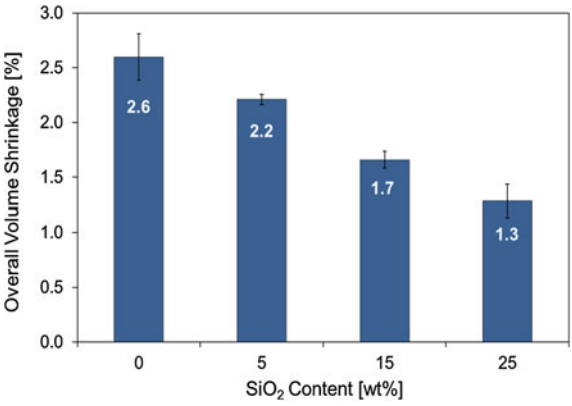


**Fig. 6.5** Overall volume shrinkage of epoxy-silica nanocomposites at RT as a function of silica content

demonstrates that an important parameter for designing or dimensioning of FRP is approximately unchanged.

Recently, the reduction of $T_g$ by nanoscaled silica was also reported by other authors, but they identified a more extensive decrease of $T_g$ [8, 9]. Mostly the effects are attributed to a reduction of crosslinking density in the polymer matrix, i.e. the chemical and physical structure of the network is significantly affected by the presence of silica nanoparticles, e.g. by the preferential adsorption of curing agent and/or low molecular weight oligomers. It is assumed in literature that the particles are surrounded by a softer polymer shell and that the strength of the polymer matrix increases with increasing distance from the surface [10]. Such interphase layers between the nanoparticles and the matrix have properties differing from those of the main matrix. However, the development of a heterogeneous network by the silica nanoparticles examined in this study seems considerably less significant. Another reason might be that the epoxy resin in the master batch is not absolutely identical with the epoxy resin used for the thinning process. Differences in the average molecular weight of the pre-polymer DGEBA also induce lower $T_g$. Therefore it has to be concluded that the presence of silica nanoparticles increases the modulus dramatically whereas the glass transition temperature is only small affected. However the mechanisms are unknown and have to be identified by a detailed analysis of the polymer-particle interfaces.

### *6.3.4 Quantitation of Resin Shrinkage*

Epoxy resins tend to build-up residual stresses induced by resin shrinkage in FRP structures [11]. Generally, high stress levels reduce the performance of FRP and should be prevented. Nanoparticles as fillers might play an important role in the reduction of resin shrinkage. Therefore the overall volume of shrinkage was

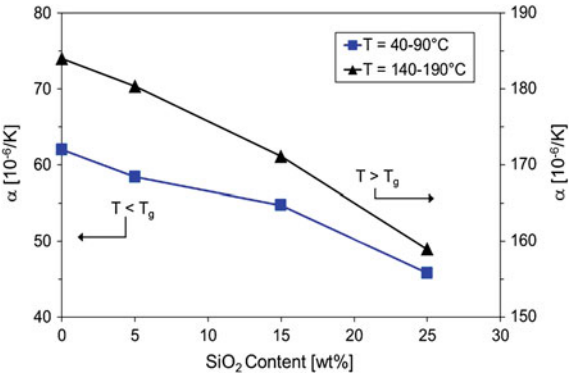


**Fig. 6.6** Linear coefficient of thermal expansion (CTE) for epoxy-silica nanocomposites as a function of the temperature range and the degree of filling (standard deviation of CTE below 5%)

determined with density measurements. Figure 6.5 shows the effect of silica nanoparticles on the course of resin shrinkage. Interestingly, the shrinkage can be reduced by approx. 50% depending on the nanoparticle content. Both the substitution of resin with non-shrinkable nanoparticles and the less exothermic character of the curing process (Table 6.1) might lead to lower shrinkage stress and internal mechanical stress in the composite which improves the suitability of the FRP (e.g. higher tolerance to damage). It should be pointed out that silica nanoparticles also decrease the coefficient of thermal expansion (CTE) as shown below and improve thermal conductivity of the polymer matrix [7]. Both parameters also affect the shrinkage process.

### 6.3.5 *Determination of Coefficients of Thermal Expansion*

Using thermo-mechanical analysis (TMA), the linear coefficients of thermal expansion were determined dilatometrically for temperature ranges both below and above $T_g$. The results are presented in Fig. 6.6 and summarized in Table 6.1. Depending on silica content and the temperature range, a significant depression in the $\alpha$-value of up to 30% is observed (form 62.0 to 45.8 $\times$ $10^{-6}$/K). This effect can be attributed to the considerably smaller CTE of the silica nanoparticles ($\alpha$ = 0.5–0.9 $\times$ $10^{-6}$/K [12]) in comparison to the significantly higher CTE of neat polymer matrix ($\alpha_{40-90°C}$ = 62.0 $\times$ $10^{-6}$/K). Moreover, the CTE might be also affected by the degree of strong interfacial properties of the nanoparticles with the epoxy resin as reported in [5]. Therefore, we can expect by the decreased CTE that resin shrinkage is reduced and the thermal stress in the composite will be smaller.

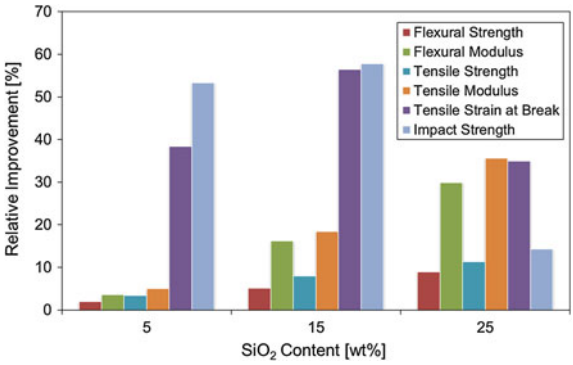


**Fig. 6.7** Relative improvements of mechanical parameters for epoxy-silica nanocomposites in relation to the neat epoxy resin and as a function of various degrees of silica filling ($G_{1c}$: +155% and $K_{1c}$: +85%; both here not listed)

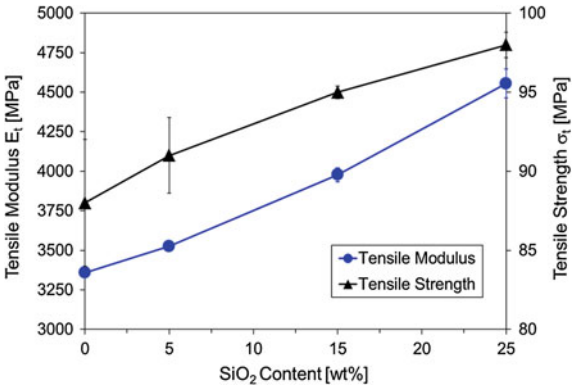


**Fig. 6.8** Tensile properties of epoxy-silica nanocomposites as a function of the silica filler content

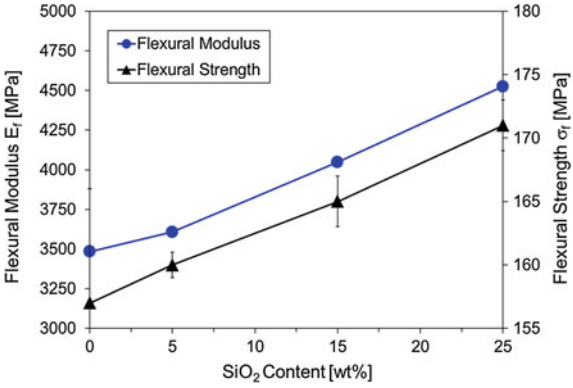


**Fig. 6.9** Flexural properties of epoxy-silica nanocomposites as a function of the silica filler content

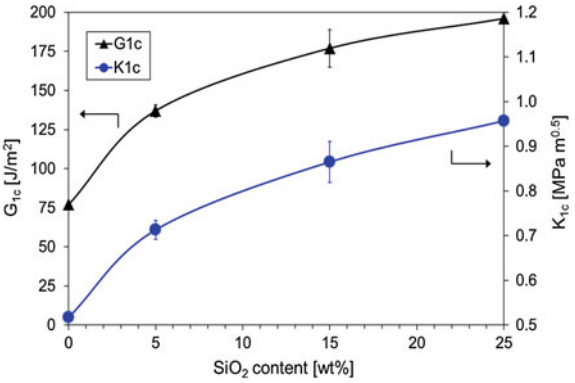


**Fig. 6.10** Facture toughness parameters of epoxy-silica nanocomposites as function of the degree of silica filling

### *6.3.6 Static Mechanical Characterization*

The improvements of the mechanical parameters of the epoxy resin by adding silica nanoparticles were investigated systematically. The absolute values are summarized in Table 6.2. The relative improvements of the mechanical properties of the nanocomposites as well as the course of absolute values for tensile, flexural and fracture toughness tests are depicted in Figs. 6.7, 6.8, 6.9, and 6.10.

The linear increase in stiffness and strength of the nanocomposites as the silica content increases is clearly distinguishable. The tensile modulus is increased by 36% and the flexural modulus by 30% at a silica content of 25 wt%. The tensile strength (ultimate) and flexural strength are increased by 11 and 9%, respectively. Interestingly, the toughness properties are also increased simultaneously as indicated by comparing the course of lines in Figs. 6.8, 6.9, and 6.10. The fracture toughness was determined by measuring the critical energy release rate ($G_{1c}$) and the critical stress intensity factor ($K_{1c}$) using compact tension test samples (CT). Both values quantify the fracture resistance at the process of crack propagation. Obviously the $G_{1c}$ and $K_{1c}$ values are improved systematically with an increased concentration of silica nanoparticles compared with the neat resin, about 155% for $G_{1c}$ and 85% for $K_{1c}$. The remarkable toughening effect is also underlined by the course of the strain at break ($\varepsilon$ (0% $SiO_2$) = 3.26%; $\varepsilon$ (15% $SiO_2$) = 5.10%) and the impact strength published in [7]. The reasons for this toughness behaviour are discussed in detail in the following chapter having a closer look at the fracture topology given by SEM und AFM images.

Furthermore, it is evident that the mechanical parameters investigated here show no maximum for the curves, which means that the mechanical maximum for this material has not been reached yet and the optimum in therms of the silica content may not yet has been adjusted. On the other hand the matrix starts to become silgthly brittle above 15 wt% silica considering the strain at break. However, this small negative effect is more than compensated by the significant increase in the stiffness, strength and toughness such that the current optimum for the

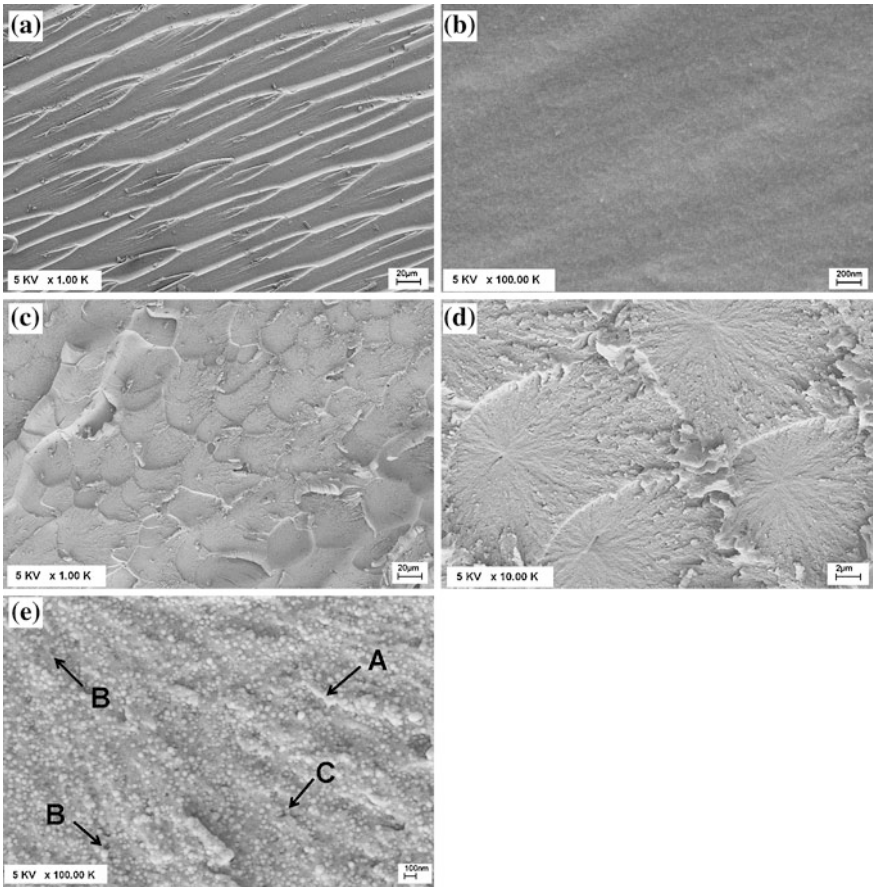


**Fig. 6.11** SEM micrographs at various magnifications for the tensile fractured surface of (**a**, **b**) the neat epoxy resin and (**c**–**e**) the epoxy-silica nanocomposites filled with 25 wt% silica. *Arrows* indicate different fracture effects: (*A*) shear banding/shear lips, (*B*) formation of cavities, (*C*) de-bonding

nanocomposite was limited to a filler content of 25 wt% silica. A further increase in the concentration of nanoparticles results in more manufacturing problems, e.g. in reduction of pot life. The slight increase in matrix density is not addressed here because it does not interfere with the lightweight construction aspect.

In this way, the strength, stiffness and toughness of the polymer matrix can be improved simultaneously by using these hard, surface functionalized silica nanoparticles i.e. the stiffness-toughness paradox seems to be solved. This effect has already been observed with some other nanoparticle systems [13] and might be attributed to a good particle–matrix interaction. A comparable improvement of

resin performance using micro-scaled fillers cannot be achieved, especially due to the much more marked brittleness effects and the reduced injectability of the resin.

### 6.3.7 Identification of Failure Mechanisms by Analysing the Fracture Surface Topology

The failure mechanism of the nanocomposites is qualitatively evaluated by SEM analysis on tensile fractured surfaces. Figure 6.11 shows SEM micrographs of the neat resin and the corresponding nanocomposite with 25 wt% silica at various magnifications.

The SEM micrograph of the neat resin shows a fracture surface at a low magnification (1000×) with river markings indicating the direction of crack propagation and rather smooth areas in between. Especially, the formation of smooth surfaces indicates the brittle behaviour of the matrix which is typical for epoxy resins. The corresponding theory of postulated failure mechanisms are summarized in the literature [14]. In contrast, the nanocomposites show a more detailed structured surface with many parabolic slices. The density of these slices also increases with increasing nanoparticle content. Although the nanoparticles are mostly homogeneously dispersed, it is assumed that the formation of slices is induced by areas with accumulated nanoparticles causing local centres of high stresses [15].

Moreover, the average roughness values ($R_a$) of the fracture surface was quantified by AFM measurements in the contact mode. Rastering of a 10 × 10 μm fracture areas reveals higher $R_a$ values for the nanocomposite (189.5 nm) than for the neat resin (48.3 nm). Figure 6.12 illustrates the different topographic profiles of the investigated samples. Obviously nanoparticles generate greater fracture areas through the development of rougher surfaces, which allows them to resist crack propagation. In consequence, the fracture energy is effectively dissipated as illustrated by the increased values of fracture toughness ($G_{1c}$; $K_{1c}$) as well as strain at break (Fig. 6.10 and Table 6.2). This leads to the conclusion that the addition of nanoparticles to the polymer matrix significantly affects the roughness of fracture surface and, in consequence, the balance between tough and brittle behaviour of the matrix.

The higher magnification of SEM micrographs (100,000 ×) reveals the formation of primary nanoparticles covered by a thin polymer shell (interlayer phase). The core–shell structure is confirmed by the large particle diameter of 50 nm compared to the average nanoparticle diameter of 16 nm measured with PCCS. Obviously these nanoparticles generate highly efficient particle–matrix interactions which is also confirmed by the observed low degree of de-bonding and pull-out effects. Accordingly the nanoparticles are well embedded in the polymer matrix and the fracture behaviour is dominated by cohesive crack propagation in the surrounding matrix. As is reported in literature, the extension of the interphase

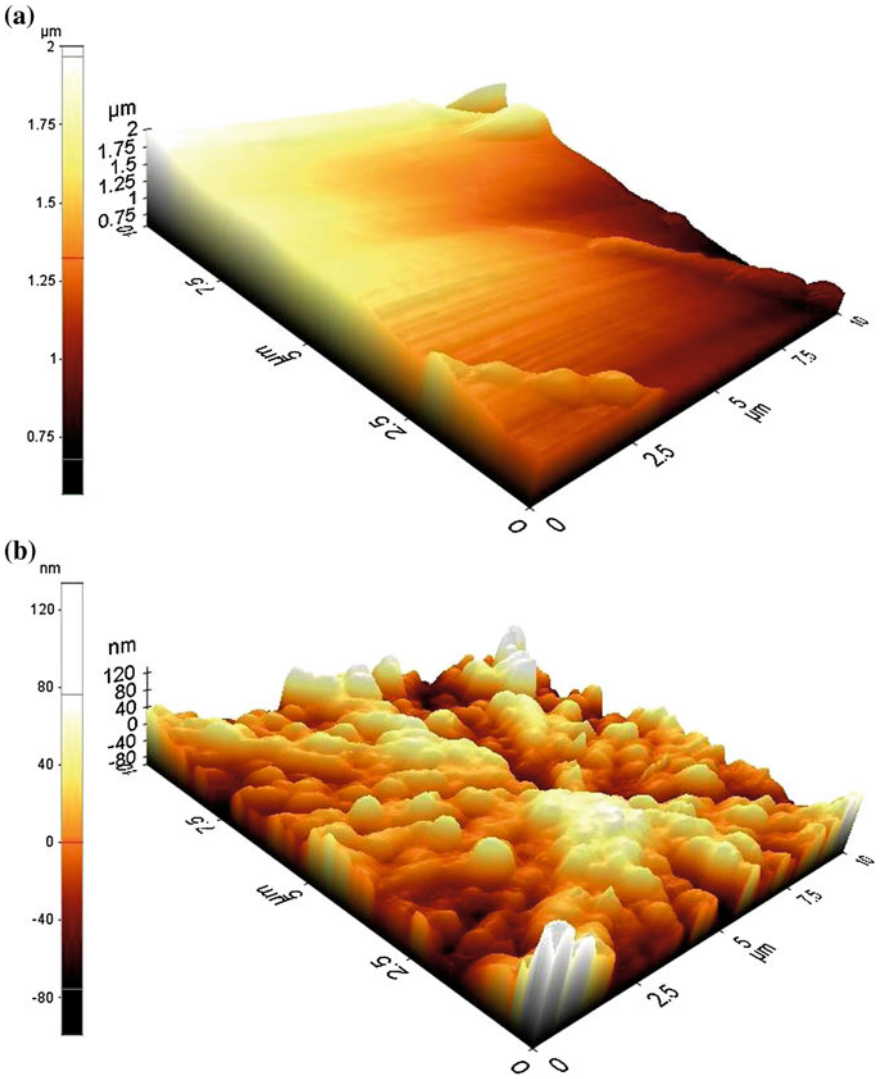


**Fig. 6.12** AFM topographic profiles of the tensile fracture surface of **a** the neat epoxy resin and **b** the corresponding epoxy-silica nanocomposites with 25 wt% silica

is proportional to the particle size [16] and is proposed to be in the range of 2–50 nm [18]. Therefore it might be expected that high degrees of filling (low interparticle distance) lead to an intersection of the particle interlayers creating the development of a strong polymer network (the bulk polymer becomes an interlayer polymer). This interpretation corresponds fairly well with the increase of stiffness

and strength as well as the improved toughening effect created with an increased silica content (Table 6.2). The influence on $T_g$ is unexpected small.

It is noteworthy that the failure mechanism seems to be a superposition of various effects. The SEM micrographs suggest shear banding and crack deflection (see arrows in Fig. 6.11). In addition particle–matrix de-bonding (voiding) and pull-out effects of particles are indicated although to a lesser extent. A more detailed interpretation of the failure mechanism is not in the scope of this paper. The influence of the interphase on the mechanical characteristics of the nanocomposite and a detailed analysis of the failure mechanism will be the focus of future research.

## 6.4 Conclusion

The paper presents the results of the investigation of epoxy-silica nanocomposites as a new type of matrix for manufacturing fiber-reinforced polymers (FRP) using injection technology (LCM). The stiffness, strength, and toughness of the composite can be significantly increased depending on the silica content compared with neat resin. These results correlate very well with the fracture surface analysis performed by means of SEM and AFM. The functionalized silica nanoparticles initiate highly profiled fracture surfaces which indicate better energy dissipation and results in increased matrix toughness. The development of core–shell structures (strong particle–matrix bonding) indicates the efficiency with which the nanoparticles are embedded in the matrix. The effective embedding might be responsible for the high levels of stiffness and strength. Moreover, the resin shrinkage and the thermal expansion coefficient are significantly reduced and the thermal conductivity increased. Therefore silica nanoparticles might entail lower shrinkage stress and also internal mechanical stress in the FRP which will extend their applicability, e.g. towards higher damage tolerance. Interestingly the silica nanoparticles seem to have slight influence on the glass transition temperature confirmed by DSC and DMA respectively. Moreover an optimum particle content of 25 wt% silica for the tested epoxy resin was identified also maintaining the injectability of these doped resins for their application in LCM processes. All in all epoxy-silica nanocomposites seem to be a new class of high performance polymer matrices for the manufacturing of FRP structures by low cost LCM techniques.

**Acknowledgments** The authors wish to thank Mr. C. Schilde (Institut of Particle Technology, Technical University Braunschweig, Germany) for AFM measurements and Dr. S. Sprenger (Hanse-Chemie AG; Geesthacht, Germany) for providing with the resin master batch.

## References


1. Rudd, C.D., Long, A.C., Kendall, K.N., Mangin, C.G.E.: Liquid Moulding Technologies. Woodhead Publishing Limited, Cambridge (1998)
2. Kruckenberg, T.K., Paton, R. (eds.): Resin Transfer Moulding for Aerospace Structures. Kluwer Academic Publisher, Dordrecht (1998)
3. Parnas, R.S.: Liquid Composite Molding. Hanser Publishers, Munich (2000)
4. Adebahr, T., Roscher, C., Adam, J.: Reinforcing nano-particles in reactive resins. Eur. Coat. J. **4**, 144–149 (2001)
5. Kang, S., Hong, S., Choe, C., Park, M., Rim, S., Kim, J.: Preparation and characterization of epoxy composites filled with functionalized nanosilica particles obtained via sol-gel process. Polymer **42**, 879–887 (2001)
6. Rosso, P., Ye, L., Friedrich, K., Sprenger, S.: A toughened epoxy resin by silica nanoparticle reinforcement. J. Appl. Polym. Sci. **100**, 1849–1855 (2006)
7. Mahrholz, T., Stängle, J., Sinapius, M.: Quantitation of the reinforcement effect of silica nanoparticles in epoxy resins used in liquid composite moulding processes. Composites: Part A **40**, 235–243 (2009)
8. Preghenella, M., Pegoretti, A., Migliaresi, C.: Thermo-mechanical characterization of fumed silica-epoxy nanocomposites. Polymer **46**, 12065–12072 (2005)
9. Zhang, H., Zhang, Z., Friedrich, K., Eger, C.: Property improvements of in situ epoxy nanocomposites with reduced interparticle distance at high nanosilica content. Acta Mater. **54**, 1833–1842 (2006)
10. Hartwig, A., Sebald, M., Kleemeier, M.: Cross-linking of cationically polymerised epoxides by nanoparticles. Polymer **46**, 2029–2039 (2005)
11. Lange, J., Toll, S., Manson, J.: Residual stress build-up in thermoset films cured below their ultimate glass transition temperature. Polymer **38**(4), 809–815 (1997)
12. Lide, D.R. (ed.): CRC Handbook of Chemistry and Physics. CRC Press, Boca Raton (2007)
13. Wetzel, B., Rosso, P., Haupert, F., Friedrich, K.: Epoxy nanocomposites—Fracture and toughening mechanisms. Eng. Fract. Mech. **73**, 2375–2398 (2006)
14. Cantwell, W.J., Roulin-Moloney, A.C.: Fractography and failure mechanisms of unfilled and particulate filled epoxy resins. In: Roulin-Moloney, A.C. (ed.) Fractography and Failure Mechanisms of Polymers and Composites, pp. 233–290. Elsevier Applied Science, London and New-York (1989)
15. Zhang, H., Zhang, Z., Friedrich, K., Eger, C.: Property improvements of in situ epoxy nanocomposites with reduced interparticle distance at high nanosilica content. Acta Mater. **54**, 1833–1842 (2006)
16. Zhong, Y., Wang, J., Wu, Y.M., Huang, Z.P.: Effective moduli of particle-filled composite with inhomogeneous interphase: Part I + II. Compos. Sci. Technol. **64**, 1345–1362 (2004)
17. Nohales, A., Munoz-Espı, R., Felix, P., Gomez, C.M.: Sepiolite-reinforced epoxy nanocomposites: thermal, mechanical, and morphological behavior. J. Appl. Polym. Sci. **119**, 539–547 (2011)
18. Schadler, L.S.: Polymer-based and polymer-filled nanocomposites. In: Ajayan, P.M., Schadler, L.S., Braun, P.V. (eds.) Nanocomposites Science and Technology. Wiley-VCH, Weinheim (2003)